Journal of Modern Optics
Vol. 00, No. 00, 1 September 2012, 1–8

arXiv:1304.4975v1 [quant-ph] 17 Apr 2013

Coupling a small torsional oscillator to large optical angular momentum

H. Shi and M. Bhattacharya*

School of Physics and Astronomy, Rochester Institute of Technology, 84 Lomb Memorial Drive, Rochester, NY 14623

(*September 28th, 2012*)

We propose a new configuration for realizing torsional optomechanics: an optically trapped windmill-shaped dielectric interacting with Laguerre-Gaussian cavity modes containing both angular and radial nodes. In contrast to existing schemes, our method can couple mechanical oscillators smaller than the optical beam waist to the in-principle unlimited orbital angular momentum that can be carried by a single photon, and thus generate substantial optomechanical interactions. Combining the advantages of small mass, large coupling, and low clamping losses, our work conceptually opens the way for the observation of quantum effects in torsional optomechanics.

Keywords: Optomechanics, Laguerre-Gaussian, Quantum, Torsional

1. Introduction

Recent advances in experimental capabilities have granted physicists access to the quantum mechanical behavior of macroscopic harmonic oscillators [1–3]. The basic paradigm underlying many of the spectacular demonstrations along this line of research stems from the interaction between a linearly vibrating mechanical object and a high finesse optical mode. Exploiting this optomechanical coupling, experimentalists have been able to measure oscillator displacement with an imprecision below the quantum limit [4, 5], engineer the quantum ground state of the oscillator [6], and discern the effects of the quantum back-action of radiation pressure [7]. A large number of theoretical proposals, targeting squeezing [8], quantum superposition [9], entanglement [10], information processing [11, 12], and exploration of the quantum-classical boundary [13] have also been put forward. In general, quantum effects are easier to detect in optomechanical systems if optical finesse, mechanical quality, mechanical frequency, and optomechanical coupling are high, and oscillator mass and ambient temperature are low [1].

In the last few years, the extension of optomechanics from linear to torsional oscillations has been considered [14–17]. This effort has been motivated by the possibility of producing rotation sensors [16], by interest in the role of photonic orbital angular momentum in manipulating matter [18], and by the desire to optomechanically address particles with more than one centre-of-mass degree of mechanical freedom [17]. Experimentally, torsional optomechanical oscillators have been presented, which however relied on linear optical momentum, which is difficult to scale up in practice [14, 16]. These oscillators also therefore did not exploit the large orbital angular momentum that can be carried by a single photon. On the theoretical front, a Fabry-Pérot design has been suggested, using spiral phase plates as end mirrors, and based on the exchange

*Corresponding author. Email: mxbsps@ rit.edu

of orbital angular momentum between the intracavity beam and one of the end plates mounted as a torsional oscillator [15]. However, it is presently difficult to produce such cavities with high finesse in the laboratory. Also, losses due to clamping introduce undesirable mechanical dissipation to the system.

A subsequent pioneering proposal brought torsional optomechanics within the realm of present experimental capabilities by theoretically considering a sub-wavelength-sized dielectric inside a standard high finesse cavity made of spherical mirrors [17]. Optical trapping of the dielectric was proposed to avoid clamping losses, while the rotational degree of freedom was addressed by Laguerre-Gaussian optical modes $LG_{l,p}$ carrying orbital angular momentum $l \neq 0$ but with a radial index $p = 0$. Couplings both linear (for cooling) and quadratic (for trapping) in the angular displacement were shown to be theoretically achievable. We show below that such couplings decrease rapidly with increasing l, requiring the impracticable use of high optical power for observing optorotational effects.

In this article, we suggest instead an optomechanical configuration that couples the torsional vibrations of a small, optically trapped, windmill-shaped dielectric to Laguerre-Gaussian $LG_{l,p}$ cavity modes carrying angular ($l \neq 0$) as well as radial ($p \neq 0$) nodes. We show that such a configuration produces, for a dielectric equal to or smaller in size than the optical beam waist, an optomechanical interaction which increases with l, provided p is chosen appropriately. The advantages of small mass, large coupling, and low clamping losses should facilitate the observation of quantum effects in the proposed system. We note that Laguerre-Gaussian beams with radial nodes have been used to rotate nanowires recently in an optical tweezer experiment [19], and also have been analyzed for tweezing efficiency [20].

2. Physical system

The physical system we propose is shown in Fig. 1. A windmill shaped object is placed inside a high finesse optical cavity and interacts with Laguerre-Gaussian modes supported by the cavity. The windmill is composed of l spokes, each of which includes two wedges with radius R, arc length s, and thickness h. The moment of inertia of the dielectric about its geometric centre is $I = lmR^2$. Such windmill rotors have been micromachined and rotated optically in the laboratory [21]. We note that the configuration suggested in Ref. [17] uses only one spoke; our proposal serves to increase the net optomechanical coupling.

We assume that the windmill is trapped in harmonic potentials axially at $z_0 \sim 0$, radially at $r_0 \sim 0$, and azimuthally at $\phi_0 \sim 0$, where the trapping frequency in the ϕ direction is ω_ϕ. The trapping can be realized with either optical tweezers [22–28] or a self-trapping scheme using modes of the optical cavity [17]. The specifics of the trapping configuration are not important for our analysis, therefore we do not discuss them in detail in the present article. The optomechanical coupling results from the interaction between the windmill and an optical field produced by the superposition of two degenerate but counter-rotating cavity modes $LG_{l,p}$ and $LG_{-l,p}$, with a beam profile given by [29]

$$|\psi_{l,p}(\mathbf{r})|^2 = A_{l,p}\frac{w_0^2}{w^2(z)}\left[\frac{r\sqrt{2}}{w(z)}\right]^{2|l|}\exp\left(-\frac{2r^2}{w^2(z)}\right)L_p^{|l|}\left[\frac{2r^2}{w^2(z)}\right]^2\cos^2 kz\cos^2 l\left(\phi-\phi'\right), \quad (1)$$

In Eq.(1), $\psi_{l,p}(\mathbf{r})$ is the optical mode function, $A_{l,p} = 2p!/[(1+\delta_{l,0})(|l|+p)!]$ is a normalization factor, $w(z) = w_0\sqrt{1+(z/z_R)^2}$ is the beam diameter, where w_0 is the beam waist, $z_R = \pi w_0^2/\lambda$ is the Rayleigh range, and λ is the wavelength of the optical radiation. Also, $L_p^{|l|}$ is an associated Laguerre polynomial, and ϕ' is the relative phase between the two modes. We note that the validity of Eq. (1) requires the Rayleigh range z_R to be larger than the cavity length L.

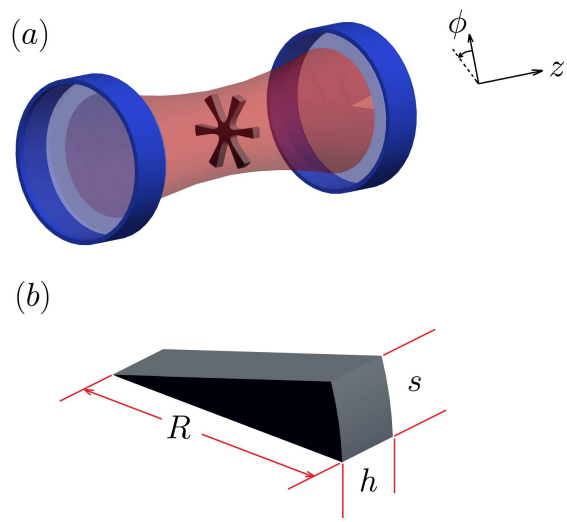

Figure 1. The physical configuration we suggest for torsional optomechanics. (a) A windmill shaped object optically trapped in a high finesse optical cavity. The object can undergo torsional oscillations along the angle labelled as ϕ. The rod is trapped near the centre of the cavity. For viewing clarity, the details of mode profile of the Laguerre-Gaussian cavity mode have not been shown here. (b) One of the wedges with its dimensions labelled.

Both the radial and the axial motions of the dielectric are completely decoupled from the windmill's azimuthal motion, and thus may be ignored. We will consider only the torsional interaction between the dielectric and the Laguerre-Gaussian beams. This interaction can be arranged to be linear in the angular displacement by choosing $\phi' = \pi/4l \sim 15^\circ$ [17], and can be modeled by the Hamiltonian [1, 30]

$$H = \hbar\omega_c(\phi_0)a^\dagger a + \hbar\omega_\phi b^\dagger b + \hbar g_{l,p} a^\dagger a(b + b^\dagger), \tag{2}$$

where $a(a^\dagger)$ and $b(b^\dagger)$ are the annihilation (creation) operators of the $\psi_{l,p}(\mathbf{r})$ mode and the mechanical mode obeying the bosonic commutation rules $[a, a^\dagger] = 1$ and $[b, b^\dagger] = 1$, respectively. The coupling constant $g_{l,p}$ in Eq. (2) can be calculated from the ϕ-dependent cavity resonant frequency $\omega_c(\phi)$, whose departure from the equilibrium value $\omega_c(\phi_0)$ due to the presence of the dielectric can be estimated using perturbation theory, since the dimensions of the dielectric are smaller than those of the beam ($s < \lambda, h < D, R \lesssim w_0/2$) [31],

$$\frac{\omega_c(\phi)}{\omega_c(\phi_0)} \simeq 1 - \frac{\int_V (\epsilon - 1)|\psi_{l,p}(\mathbf{r})|^2 d\mathbf{r}}{2\int_{V'} |\psi_{l,p}(\mathbf{r})|^2 d\mathbf{r}}, \tag{3}$$

where ϵ and V are the dielectric constant and volume, respectively, of the windmill, and V' is the volume of the whole cavity. The optomechanical coupling in Eq. (2) can then be found as $g_{l,p} = \sqrt{\hbar/I\omega_\phi}\partial\omega_c(\phi)/\partial\phi|_{\phi_0}$ from Eq. (3).

3. Laguerre-Gaussian modes without radial nodes

In this section, we consider the optomechanical coupling $g_{l,p}$ in detail. We first assume $l \neq 0, p = 0$, which corresponds to a beam profile without radial nodes. Generalizing the treatment

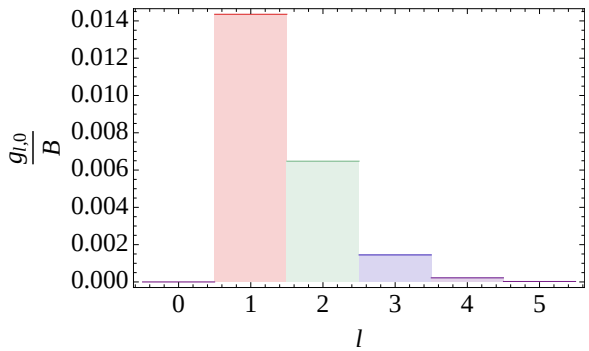

Figure 2. (Color online) Plot of the optomechanical coupling [Eq. (4)], between the dielectric windmill of Fig. 1 and the optical mode of Eq. (1) for $R/w_0 = 1/2, p = 0$, and various l.

of Ref. [17] to arbitrary l, we find

$$\frac{g_{l,0}}{B} = \frac{\Gamma\left[|l|+1\right] - \Gamma\left[|l|+1, 2\left(\frac{R}{w_0}\right)^2\right]}{|l|^{-1}(|l|-1)!(1+\delta_{l,0})}, \tag{4}$$

where $\Gamma[|l|+1]$ is the complete and $\Gamma[|l|+1, 2R^2/w_0^2]$ the incomplete Gamma function, and $B = (\epsilon - 1)(wt/\pi RD)\omega_c(\phi_0)\sqrt{\hbar/mR^2\omega_\phi}$ is a constant independent of l. Choosing $R/w_0 = 1/2$ as in Ref. [17], we see from Fig. 2 that $g_{l,0}/B$ decreases dramatically with l. This behavior can be understood from the simple fact that the single radial maximum of the $|\psi_{l,p=0}(\mathbf{r})|^2$ mode profile near $z \sim 0$ lies at $r_{\max}^{|l|} \simeq w_0\sqrt{|l|/2}$ [32]. Thus, for higher values of l the radiation is too far away from the beam centre ($r_{\max}^{|l|} \gg R$) to couple to any dielectric equal to or smaller than the beam waist ($R \lesssim w_0/2$). Such a dielectric therefore experiences mostly the dark core of the optical mode. This situation has been depicted in Fig. 3, which shows a cross-section of the cavity at $z = 0$ in the $x - y$ plane. Clearly, the windmill overlaps very little with the six intensity maxima for the $l = 3, p = 0$ beam shown using solid curves.

One way of coupling to higher l modes is, of course, to increase proportionately the radius R of the windmill. However, the corresponding increase in mass would make the observation of quantum effects, as well as optical trapping, more challenging; the increase in surface area would lead to larger mechanical damping rates due to collisions with background gas molecules; and the increase in size would lead to more optical scattering due to diffraction, reducing the finesse of the cavity. For these reasons, we consider it important to find a technique for strengthening the optomechanical coupling without using dielectrics with diameter larger than the optical beam waist w_0(a parameter which can be held constant as l is increased). Below, we suggest such a method.

4. Laguerre-Gaussian modes with radial nodes

Consider now a situation in which $l \neq 0, p \neq 0$. Laguerre-Gaussian cavity modes with p up to 12 and l up to 28 have been produced experimentally [33]. In this case, $g_{l,p}/B$ could be calculated only numerically for arbitrary l and p, and is displayed in Fig. 4 [1]. This figure shows two clear trends. First for every l, there is a value of p at which the coupling reaches a maximum. Second, and in sharp contrast to Fig. 2, the magnitude of this maximum increases with l. These characteristics can be broadly understood from Fig. 3, which displays the thirty six intensity

[1]We note that $g_{l,p}/B$ can be calculated analytically for any given l, and arbitrary p.

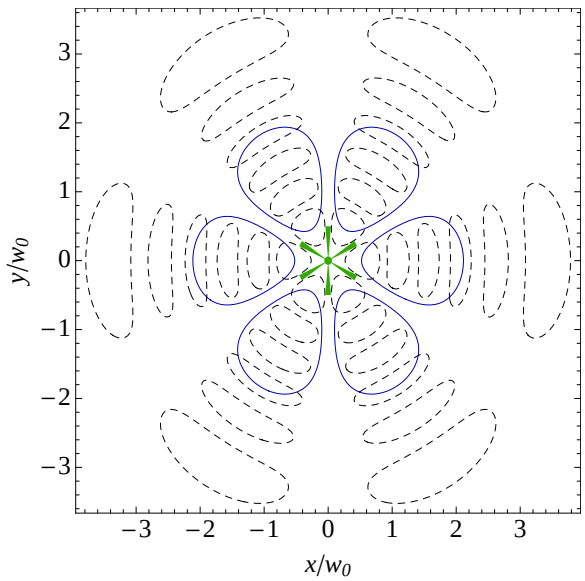

Figure 3. (Color online) A cross-section of the cavity of Fig. 1 at $z = 0$, showing the windmill dielectric and the optical modes (with a beam waist of w_0) it interacts with. The intensity maxima drawn with solid lines correspond to Eq. (1) with $l = 3, p = 0$, while the lobes drawn using dashed lines correspond to Eq. (1) with $l = 3, p = 5$. For clarity of viewing, $\phi' = 0$ has been used in both cases.

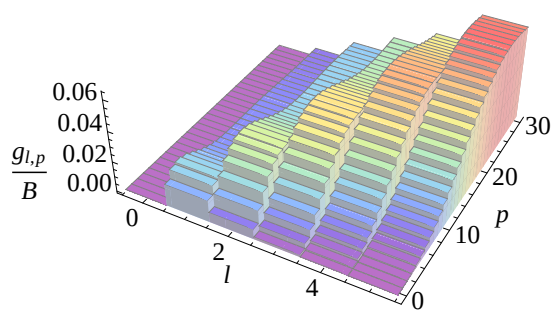

Figure 4. (Color online) Plot of the optomechanical coupling $g_{l,p}/B$, between the dielectric windmill of Fig. 1 and the optical mode of Eq. (1) for $R/w_0 = 1/2$, and various l and p.

maxima of the $l = 3, p = 5$ beam as dashed curves. Clearly, for larger p, the six innermost lobes of the beam overlap better with the dielectric, leading to an increase in the optomechanical coupling. However, the appearance of thirty additional lobes results in loss of intensity from the innermost maxima, thus weakening the coupling with the dielectric. The competition between these two opposing mechanisms yields, for a given l, an optimum $g_{l,p}$ at a particular value of p. For $l = 3$, for example, the peak in the coupling occurs at $p = 11$, as can be seen from Fig. 4. For higher values of l, the maximum coupling is stronger, since the slope of the mode profile $|\psi_{l,p}(\mathbf{r})|^2$ near the angular equilibrium position is sharper along ϕ in this case.

Assuming that the windmill is machined from fused silica, and using parameters from relevant experiments [34, 35] and experimental proposals [17] ($D = 0.5$ mm, $\lambda = 1064$ nm, $w_0 = 20$ μm, $l = 3, p = 11$, $\epsilon = 2.1$, $m = 10^{-16}$ kg, $R = 10$ μm, $s = h = 200$ nm, $\omega_\phi = 50$ kHz), we find $g_{3,11} \sim 200$ Hz. This is much larger than the coupling for a $p = 0$ beam, $g_{3,0} \sim 5$ Hz. Clearly, the presence of radial nodes increases the coupling dramatically. Further, reducing the radius to $R = 8$ μm we find a coupling of 100 Hz by using $l = 3$ and $p = 15$. The method we have suggested can therefore be used in principle for dielectrics of the size of the beam waist or smaller.

In practice, the waist of a diffraction-limited optical beam is of the order of a few wavelengths, i.e. a few microns. For comparison, optomechanical experiments have involved dielectric particles ranging in size from tens of nanometers [34] to a few microns [35]. With currently available $LG_{l,p}$ modes, our technique should be able to address particles at the upper limit of such length-scales.

Before concluding this section we make two observations. Our first comment relates to our choice of a windmill shape for the dielectric. If the fabrication of the windmill proves to be difficult for high l (i.e. large number of spokes), it can be substituted by a single rod, as in Ref.[17]. We have found that in this case the presence of radial nodes in the optical mode yields an optomechanical coupling whose behavior with l is qualitatively the same as for the windmill, although its magnitude is reduced somewhat, as may be expected. Second, we note that optomechanical couplings quadratic in ϕ, which increase with l, are also achievable using our method, by setting $\phi' = 0$ in Eq. (1). The extension of the self-trapping scheme of Ref. [17] to beams containing radial nodes would in fact be useful to optically confine torsionally oscillating dielectrics such as presented in this article.

5. Decoherence

From the perspective of quantum applications, it is relevant to consider the decoherence of the dielectric due to mechanisms such as photon scattering. The decoherence rate of the dielectric due to the scattering of photons out of the cavity can be calculated using a master equation approach [36]. In Ref. [36], the decoherence rate $\Gamma^{\rm cav}$ was calculated for a dielectric sphere with radius up to twice the optical wavelength. We have extended the calculation to a dielectric sphere with radius up to ten times the optical wavelength. For a sphere of this size, geometrical scattering predominates. In order to adapt the decoherence calculation for the sphere to our geometry, we need to account for the fact that our system is composed of a dielectric windmill, which has a much smaller cross sectional area than a sphere of comparable radius. Also, our proposal involves Laguerre-Gaussian beams, which have several radial and azimuthal intensity minima, as compared to a Gaussian beam considered in the case of the sphere. These factors are expected to reduce the photon scattering rate as compared to dielectric spheres in Gaussian beams, and can be accounted for by multiplying $\Gamma^{\rm cav}$ by the following geometric ratio

$$\zeta_{l,p} = \frac{\int_{A_w} |\psi_{l,p}(\mathbf{r})|^2 da}{\int |\psi_{l,p}(\mathbf{r})|^2 da}, \tag{5}$$

where A_w is the geometric cross sectional area of the windmill. Multiplying the decoherence rate for the sphere with this dimensionless geometric factor, we obtain a decoherence rate

$$\Gamma_{l,p} = \zeta_{l,p}\Gamma^{\rm cav}. \tag{6}$$

This decoherence rate is shown in Fig. 5, for the same ranges of l and p as in Fig. 4. We find that typically $\Gamma_{l,p} \simeq 1$Hz, much smaller than the coherent coupling rate of $g_{l,p} \simeq 100$Hz demonstrated above. We note here that the optomechanical coupling depends on the relative volumes of the dielectric and the optical mode [Eq. (3)], while the photon scattering rate is governed by the ratio of their transverse areas [Eq. (6)] Fig. 4. The key point of course is that the rate of decoherence is small compared to the coherent coupling in the regime of interest, making our proposal feasible.

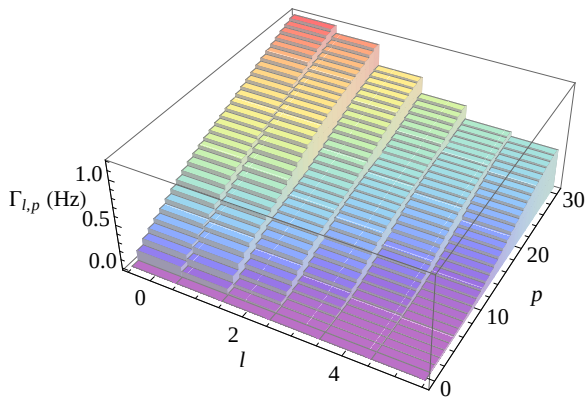

Figure 5. (Color online)Plot of the decoherence rate $\Gamma_{l,p}$, due to photon scattering from the trapping beam by the dielectric windmill of Fig. 1 from the optical mode of Eq. (1) for $R/w_0 = 1/2$, and various l and p. The power in the trapping beam incident on the cavity is 0.1mW [36, 37].

6. Conclusion

In this article we have suggested a new torsional optomechanics configuration using the interaction between an optically trapped "windmill"-shaped dielectric and a superposition of two counter rotating Laguerre-Gaussian modes. We have demonstrated that the in-principle unlimited angular momentum carried by a photon can be harnessed to dielectrics smaller than the beam waist if the number of radial nodes in the optical mode is chosen appropriately. We have shown that this scheme can provide sizable optomechanical interactions using realistic experimental parameters. Featuring small mass, large coupling, and low clamping losses, our proposal paves the way for exploring quantum effects in torsional optomechanics.

Acknowledgements

We thank Dr. S. Preble and Dr. E. Hach III for useful discussions and the Research Corporation for Science Advancement for support.

References

[1] Kippenberg, T.J.; Vahala, K.J. Cavity Optomechanics: Back-Action at the Mesoscale. *Science* **2008**, *321* (5893), 1172–1176.
[2] Marquardt, F.; Girvin, S.M. Optomechanics. *Physics* **2009**, *2*.
[3] McClelland, D.E.; Mavalvala, N.; Chen, Y.; et al. Advanced interferometry, quantum optics and optomechanics in gravitational wave detectors. *Laser and Photonic Reviews* **2011**, *5* (677-696).
[4] Teufel, J.D.; Donner, T.; Castellanos-Beltran, M.A.; Harlow, J.W.; et al. Nanomechanical motion measured with an imprecision below that at the standard quantum limit. *Nature Nanotechnology* **2009**, *4*, 820–823.
[5] Braginsky, V.B. Quantum Measurement. : , 1995.
[6] Chan, J.; Alegre, T.P.M.; Safavi-Naeini, A.H.; Hill, J.T.; Krause, A.; Gröblacher, S.; Aspelmeyer, M.; et al. Laser cooling of a nanomechanical oscillator into its quantum ground state. *Nature* **2011**, *478*, 89–92.
[7] Brahms, N.; Botter, T.; Schreppler, S.; Brooks, D.W.C.; et al. Optical Detection of the Quantization of Collective Atomic Motion. *Physical Review Letters* **2012**, *108* (13).
[8] Nunnenkamp, A.; Børkje, K.; Harris, J.G.E.; et al. Cooling and squeezing via quadratic optomechanical coupling. *Physical Review A* **2010**, *82* (2).
[9] Kleckner, D.; Pikovski, I.; Jeffrey, E.; Ament, L.; Eliel, E.; van den Brink, J.; et al. Creating and verifying a quantum superposition in a micro-optomechanical system. *New Journal of Physics* **2008**, *10*.
[10] Vitali, D.; Gigan, S.; Ferreira, A.; Böhm, H.R.; Tombesi, P.; Guerreiro, A.; Vedral, V.; Zeilinger, A.; et al. Optomechanical Entanglement between a Movable Mirror and a Cavity Field. *Physical Review Letters* **2007**, *98* (3).
[11] Mancini, S.; Vitali, D.; Tombesi, P. Scheme for Teleportation of Quantum States onto a Mechanical Resonator. *Physical Review Letters* **2003**, *90* (13).
[12] Stannigel, K.; Komar, P.; Habraken, S.J.M.; Bennett, S.D.; Lukin, M.D.; Zoller, P.; et al. Optomechanical Quantum Information Processing with Photons and Phonons. *Physical Review Letters* **2012**, *109* (1).

[13] Romero-Isart, O.; Pflanzer, A.; Blaser, F.; Kaltenbaek, R.; Kiesel, N.; Aspelmeyer, M.; et al. Large Quantum Superpositions and Interference of Massive Nanometer-Sized Objects. *Physical Review Letters* **2011**, *107* (2).
[14] Tittonen, I.; Breitenbach, G.; KalkBrenner, T.; Müller, T.; Conradt, R.; et al. Interferometric measurements of the position of a macroscopic body: Towards observation of quantum limits. *Physical Review A* **1999**, *59* (2), 1038–1044.
[15] Bhattacharya, M.; Meystre, P. Using a Laguerre-Gaussian Beam to Trap and Cool the Rotational Motion of a Mirror. *Physical Review Letters* **2007**, *99* (153603).
[16] Mueller, F.; Heugel, S.; Wang, L.J. Observation of optomechanical multistability in a high-Q torsion balance oscillator. *Physical Review A* **2008**, *77* (3).
[17] Romero-Isart, O.; Juan, M.L.; Quidant, R.; et al. Toward quantum superposition of living organisms. *New Journal of Physics* **2010**, *12*.
[18] Torres, J.P.; Torner, L. (Eds.), Twisted Photons. : , 2011.
[19] Shi, L.; Li, J.; Tao, T.; et al. Rotation of nanowires with radially higher-order Laguerre–Gaussian beams produced by computer-generated holograms. *Applied Optics* **2012**, *51*, 6398–6402.
[20] Chai, H.S.; Wang, L.G. Improvement of optical trapping effect by using the focused high-order Laguerre-Gaussian beams. *Micron* **2012**, *43*.
[21] Galajda, P.; Ormos, P. Rotation of microscopic propellers in laser tweezers. *Journal of Optics B: Quantum and Semiclassical Optics* **2002**, *4* (2).
[22] Kong, L.; Zhang, P.; Wang, G.; Yu, J.; Setlow, P.; et al. Characterization of bacterial spore germination using phase-contrast and fluorescence microscopy, Raman spectroscopy and optical tweezers. *Nature Protocols* **2011**, *6*, 625–639.
[23] Cheung, H.K.; Law, C.K. Optomechanical coupling between a moving dielectric sphere and radiation fields: A Lagrangian-Hamiltonian formalism. *Physical Review A* **2012**, *86* (3).
[24] Chang, D.E.; Regal, C.A.; Papp, S.B.; Wilson, D.J.; Ye, J.; Painter, O.; Kimble, H.J.; et al. Cavity optomechanics using an optically levitated nanosphere. *Proceedings of Natioanl Academy of Science* **2009**.
[25] Singh, S.; Phelps, G.A.; Goldbaum, D.S.; Wright, E.M.; et al. All-Optical Optomechanics: An Optical Spring Mirror. *Physical Review Letters* **2010**, *105* (21).
[26] Barker, P. Doppler Cooling a Microsphere. *Physical Review Letters* **2010**, *105* (7).
[27] Schulze, R.; Genes, C.; Ritsch, H. Optomechanical approach to cooling of small polarizable particles in a strongly pumped ring cavity. *Physical Review A* **2010**, *81* (6).
[28] qi Yin, Z.; Li, T.; Feng, M. Three-dimensional cooling and detection of a nanosphere with a single cavity. *Physical Review A* **2011**, *83* (1).
[29] Siegman, A.E. Lasers. : , 1986.
[30] Bhattacharya, M.; Meystre, P. Trapping and Cooling a Mirror to Its Quantum Mechanical Ground State. *Physical Review Letters* **2007**, *99* (7).
[31] Johnson, S.G.; Ibanescu, M.; Skorobogatiy, M.A.; Weisberg, O.; Joannopoulos, J.D.; et al. Perturbation theory for Maxwell's equations with shifting material boundaries. *Physical Review E* **2002**, *65* (066611).
[32] Arlt, J.; Kuhn, R.; Dholakia, K. Spatial transformation of Laguerre-Gaussian laser modes. *Journal of Modern Optics* **2001**, *48* (5), 783–787.
[33] Thirugnanasambandam, M.P.; Senatsky, Y.; Ueda, K. Generation of very-high order Laguerre-Gaussian modes in Yb:YAG ceramic laser. *Laser Physics Letters* **2010**, *7* (9), 637–643.
[34] Gieseler, J.; Deutsch, B.; QUidant, R.; et al. Subkelvin Parametric Feedback Cooling of a Laser-Trapped Nanoparticle. *Physical Review Letters* **2012**, *109* (10).
[35] Li, T.; Kheifets, S.; Raizen, M.G. Millikelvin cooling of an optically trapped microsphere in vacuum. *Nature Physics* **2011**, *7*, 527–530.
[36] Pflanzer, A.C.; Romero-Isart, O.; Cirac, J.I. Master-equation approach to optomechanics with arbitrary dielectrics. *Physical Review A* **2012**, *86*, 013802.
[37] Lechner, W.; Habraken, S.J.M.; Kiesel, N.; Aspelmeyer, M.; et al. Cavity optomechanics of levitated nano-dumbells: Non-equilibrium phases and self-assembly. *arxiv:1212.4691* **2013**.